AERIAL IMAGE BASED GEOMETRIC REFINEMENT OF BUILDING MODELS DERIVED FROM AIRBORNE LIDAR DATA

M. Jarząbek-Rychard [a,b] *, H-G. Maas [b]

[a] Institute of Geodesy and Geoinformatics, Wroclaw University of Environmental and Life Science, Poland - malgorzata.jarzabek-rychard@igig.up.wroc.pl
[b] Institute of Photogrammetry and Remote Sensing, Technische Universität Dresden, Germany - hans-gerd.maas@tu-dresden.de

KEY WORDS: building reconstruction, 3D modeling, laser scanning, aerial imagery, edge matching

ABSTRACT:

Airborne laser scanning has proven to be a strong basis for the automatic generation of 3D building models. A drawback, however, is often in the point spacing of typical datasets. As a consequence, the precision of roof plane and ridge line parameters is usually significantly better than the precision of gutter lines. To cope with problem the paper presents a novel approach for geometric refinement of building models reconstructed from ALS point clouds using single aerial imagery. The basis idea of our modeling approach it to obtain refined roof corners by direct intersection of 3D roof planes previously extracted from ALS data with viewing planes assigned with the edges detected in high resolution digital photographs. The synergy between LiDAR and optical imagery allows for obtaining building models with high vertical and plannimetric accuracy. In order to evaluate performance of our refinement algorithm, we compare the results of 3D reconstruction executed using only laser scanning data and enhanced by image information. Furthermore, quality assessment of both modeling outputs is performed based on a reference data provided by the ISPRS benchmark for 3D building reconstruction. Integration of linear cues retrieved from single imagery allows for average improvement of planar accuracy of 9 cm (RMS error for roof plane outlines). The overall quality of final building models calculated on a per-area level reaches nearly 90%.

1. INTRODUCTION

Accurate and timely updated 3D building models has been considered a critical element of urban scene reconstruction. Virtual models serve as an important information source to support various domains such as urban planning, disaster management, navigation and tourism. Permanently increasing spectrum of applications urgently demands advanced methods for efficient and highly automatized reconstruction algorithm providing up-to-date products. Despite worldwide intensive efforts to improve the modeling process, reconstruction of highly accurate building models still remains as a challenging task (Rottensteiner et al., 2014).

Due to the needs for efficient modeling covering large areas the base information for building extraction mainly comes from airborne data: laser scanning and imagery. For the past two decades numerous research papers concerning building reconstruction were published, which used LiDAR data (e.g. Oude Elberink and Vosselman, 2009; Kim and Shan, 2011; Xiong et al., 2015) or image information (Nex and Remondino, 2012; Bulatov et al., 2014). Airborne laser scanning has proven to be a strong basis for the automatic generation of 3D building models. Vertical accuracy of the reconstructed rooftops is adequate even for highly demanding engineering applications. Unfortunately, building models derived from ALS point clouds are restricted by the ground resolution of datasets. Hence it is difficult to achieve high planimetric accuracy of a reconstructed scene. Compared to laser scanning, optical imagery with its higher spatial resolution usually allows for a more accurate extraction of building edges, accompanied by a higher precision of reconstructed 3D elements. Largely complementary nature of LiDAR and image data forms a basis for an efficient combination of these two techniques. Integration of laser scanning and imagery for 3D reconstruction can be performed in two ways, using parallel or sequential approach (Sohn et al., 2013). In case of the former one, each modeling cues is extracted from two datasets at the same time (Chen et al., 2005; Habib et al., 2011; Demir and Baltasavias, 2012; Zhang et al., 2014). In the sequential fusion approach, building models are generated based on a single information source and later refined by the other data (Perera, 2014; Dal Poz, 2014). The latter method may also depict an opportunity for an effective update of virtual cities already reconstructed from LiDAR. In these terms, existing 3D models can serve as an input for improving their accuracy by newly collected information.

This paper presents a novel approach for sequential refinement of 3D building models using a single aerial image. The core idea of modeling improvement it to obtain refined model edges by intersecting roof planes accurately extracted from 3D point clouds and viewing planes assigned with building edges detected in a high resolution aerial image. Although 3D models reconstructed from LiDAR show deficits in their planimetric accuracy, they serve as a good input information for structural arrangements of roofs and convergence priors. In order to improve the geometric accuracy of roof plane outlines, 3D roof edges are projected into image space and substituted by the best matching linear segments extracted from the image. The chosen lines are projected back to 3D space and intersected with relevant planes previously detected from ALS data. The underlying methodology so far assumes that the input models are topologically correct. The research aim is then to increase the geometric accuracy of reconstructed roofs. In order to evaluate performance of our refinement algorithm, we compare the results of 3D reconstruction performed only using ALS data

* Corresponding author,

and enhanced by information retrieved from an aerial image. Furthermore, quality assessment of both modeling outputs is performed based on a comparison to the reference data, according to the validation methods standardized by the International Society for Photogrammetry and Remote Sensing (Rutzinger et al., 2009).

2. REFINEMENT METHODOLOGY

2.1 Projection of a 3D model to the image space

3D building models previously reconstructed from an ALS point cloud provide structural arrangements of roofs and convergence priors. Initial models subjected to the refinement are reconstructed according to the approach described in Jarząbek-Rychard and Borkowski, 2016) and stored as a list of *x,y,z* coordinates of roof vertices and their topological relations (connecting edges). The first step of the implemented algorithm is to project an input wireframe model into image space. The projection is performed through the collinearity equations, along with known exterior and interior orientation parameters. First, object space points (3D roof vertices) are transformed into the camera coordinate system. In the second step, the internal camera model and the interior orientation parameters are used to transform camera points into the image space. Finally, projected 2D points are connected according to the topology information provided by input models. As a result (c.f. Fig.1a), initial 3D building boundaries are transformed into planar lines and thus, integrated in the image.

2.2 Linear feature extraction

To automatically extract straight line segments from aerial photographs we use the Canny edge detector followed by connected component analyses and Hough transform. The result of Canny operator (presented in Fig.1b) is a binary image with marked edge pixels associated to object boundaries. Straight line segments and related line equations are computed by finding peaks in the Hough space of the binary image. According to the assumption underlying Hough transform, the pixels lying on one line need not all be contiguous. This fact can give misleading results when different objects happen to be aligned by chance. Thus, in order to reduce the searching space for potential pixels belonging to the estimated line, we use connected component labelling (c.f. Fig.1c). The labelling is applied to the boundary image provided by the Canny edge detector. Hough transform is then repeated for each binary image assigned to one connected components (detected straight lines are shown in Fig.1d). Besides building edges, extracted information is also related to other, irrelevant objects such as vegetation, fences, or roof patterns. On the other hand, some desired roof boundaries may not be derived due to shadow areas and occlusions. Hence, all the extracted linear features are treated as sharp boundary information and serve as an input for correspondence matching, performed in the next step.

2.3 Similarity measure and line matching

Similarity measures are defined to find correspondences between projected lines of a 3D model and new edges extracted from the image. The aim of line matching is to substitute each building edge initially reconstructed from ALS by the best candidate chosen from the line segments extracted by image processing. At this stage of refinement procedure both edge sets, reference and candidate, follow the same pixel coordinate system. Hence, it is possible to compute mutual geometric relationships and find corresponding pairs of boundary lines. The matching algorithm involves the following criteria to choose the correct image line for each reference edge:

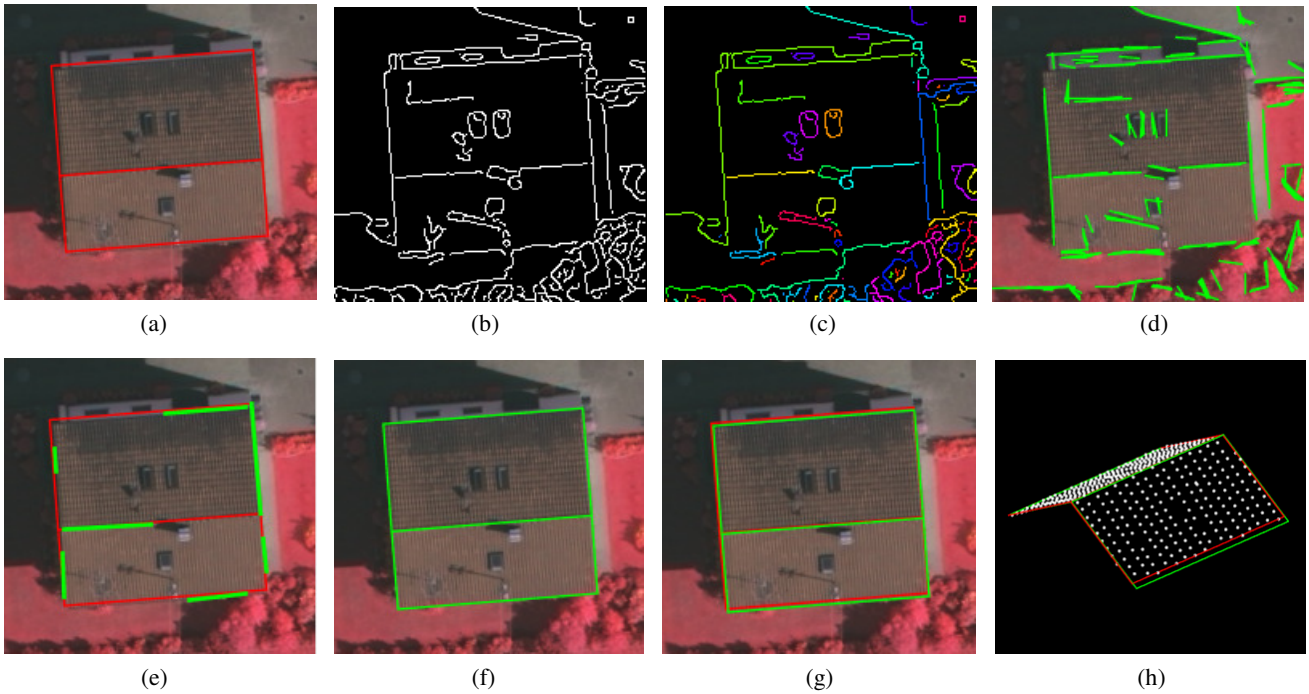

(a) (b) (c) (d)

(e) (f) (g) (h)

Figure 1. Refinement process: input wireframe model projected into image space (a), extracted boundary image (b), connected component labelling (c), straight lines detected by Hough transform (d), correspondence matching; if no new line is matched then the input line is preserved (e), refined wireframe model projected into the image (f), comparison of building models before (red) and after (green) refinement – image space (g), comparison of building models before and after refinement – 3D space (h).

- proximity of both lines defined by the distances from both end-points of a candidate segment to a reference line segment,
- similar orientation defined by the angle between reference and candidate line,

If there is more than one line fulfilling the two requirements above, the closest line is chosen.

Several factors, such as shadows along the desired edge, poor contrast, occlusions, or erroneous references can hinder proper extraction of all relevant building edges. Hence, it is not always possible to find a corresponding line for each reference edge. In this case, the 2D equation of an initial edge is used in further processing. Figure 1e presents ALS-based building edges and their best matching lines detected from the image. Newly extracted roof edges are rectified and aligned perpendicular or parallel to the main orientation of a building. Because orientation of a ridge line derived from ALS is expected to reach high accuracy, it determines the dominant building direction. For building types that do not include ridge lines (e.g. flat roofs) detected lines are regularly aligned with respect to the longest matched line detected in the image.

2.4 Reconstruction of a refined 3D model

A refined 3D building model is generated by the intersection of roof planes extracted from ALS data with viewing planes assigned with newly detected edges. In order to reconstruct viewing planes, viewing ray vectors are generated for both end points of a 2D line. A viewing plane is then created based on the plane normal derived by the cross product of viewing ray vectors and coordinates of the projection center. Intersection of neighboring viewing planes and 3D planes of a roof enables to obtain refined 3D coordinates of roof corners. The neighboring planes are identified according to the topology information stored in the input building models. In the final step of building reconstruction 3D models are subjected to the regularization. As a result, right angles of boundary edges are preserved and 3D lines assigned to ridges and gutters are aligned horizontally. The refined building model projected back to the image space is shown in Fig.1f. Finally, wireframe models constructed before and after refinement are compared in the image space (c.f. Fig.1g) and 3D space (c.f. Fig.1h).

3. RESULTS AND DISCUSSION

To verify the performance of the presented approach we used data provided by ISPRS WGIII/4 (Rottensteiner et al., 2014). The dataset (area3 – Vaihingen) presents a purely residential area with 56 detached houses. The ALS point cloud was collected by Leica ALS50 system with a density of 4 points / m^2. The aerial images were acquired using an Intergraph / ZI digital mapping camera with a ground sampling distance of 8 cm and a radiometric resolution of 12 bits. The interior and exterior parameters were determined in the level of one pixel georeferencing accuracy. The refinement method was applied to a set of 3D building models generated on LoD2 (Jarząbek-Rychard and Borkowski, 2016). An overview on the results of our experiment is presented in Fig.1. The both sets of 3D building models, reconstructed from ALS data only and enhanced by image information, are transformed into the image 2D space and compared.

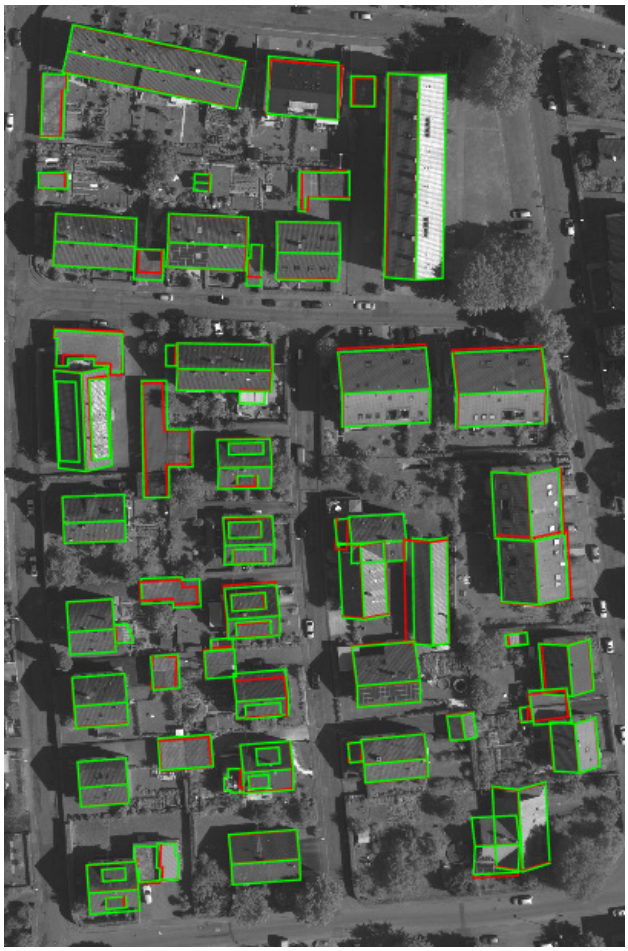

Figure 1. Reconstructed 3D models projected into the image: roof edges generated from ALS point clouds (red) and refined using single aerial imagery (green) (for better visibility in this figure original infrared image is transformed into gray scale).

Edge type	# edges	mean shift [cm]
ridge	34	5,5
gutter	68	17,9
eave	136	13,1
dormer	56	21,1
flat	94	43,3
height jump	10	54,4
adjacent flat	30	12,2

Table 1. Quantitative analysis of the refinement performance: mean planar displacement of building edges.

To get a clear idea of the influence of the applied refinement procedure an average planar displacement of different types of roof edges is calculated. For that reason we computed perpendicular distance between each reference ALS edge line and the end-points of a corresponding line extracted from the image. Table 1 shows quantitative analysis of the resulting changes presented with respect to the edge type. The statistics are illustrated in Fig. 2.

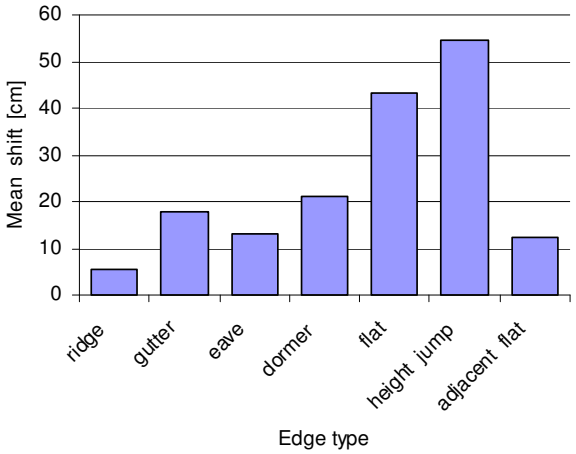

Figure 2. Mean planar displacement of building edges presented with respect to the edge type.

The largest displacement (54 cm) is shown for height jump edges. Such situations result from a limitation of the applied building reconstruction method, in which a gap may arise between a single roof and its adjacent multi roof plane building. The integrated image information allows for a compensation of this effect by shifting the lower height jump edge to the planar position of the upper one. The second biggest change of planar position (43 cm) is observed for the outlines of flat roofs, which are sensitive to ALS point spacing and directional arrangements of scanning lines. Interestingly, small roofs adjacent to complex buildings, which are also usually flat-type, show much smaller displacement (12 cm). Such roofs are usually significantly smaller and often affected by shadows. Thus, it is difficult to extract a correct matching line from the image. As expected, the smallest change after applied refinement (about 5 cm shift) is noted for ridge lines, which are precisely determined from ALS data by an intersection of 3D planes.

Input data	ALS	ALS & image
RMS (reference boundaries) [cm]	73	64
Evaluation on a per-area level:		
True Positives [m^2]	7430,5	7522,5
False Positives [m^2]	276,5	262,0
False Negatives [m^2]	683,9	591,9
True Negatives [m^2]	33609,1	33623,5
Completeness [%]	91,6	92,7
Correctness [%]	96,4	96,6
Quality [%]	88,6	89,8

Table 2. Qualitative assessment of roof location accuracy performed with respect to the reference data. Integration of linear features extracted from aerial image improves the rate of all performance indicators.

In order to asses the quality of the reconstructed 3D models, both sets of the modeling results (before and after correction) were verified within ISPRS Test Project on Urban Classification and 3D Building Reconstruction. The benchmark allows for the evaluation of the modeling results according to unified criteria against other reconstruction methods. The statistics on qualitative analysis concerning plannimetric accuracy of roof plane outlines are collected in Tab.2. Since all the indicators are improved, it can be stated that the integration of refinement procedure certainly increases the modeling performance. The assumption of the refinement approach preserves initial roof structure of a model. Therefore, only the 3D position of roof corners is modified. As no new building components can appear in the refined scene, the overall quality

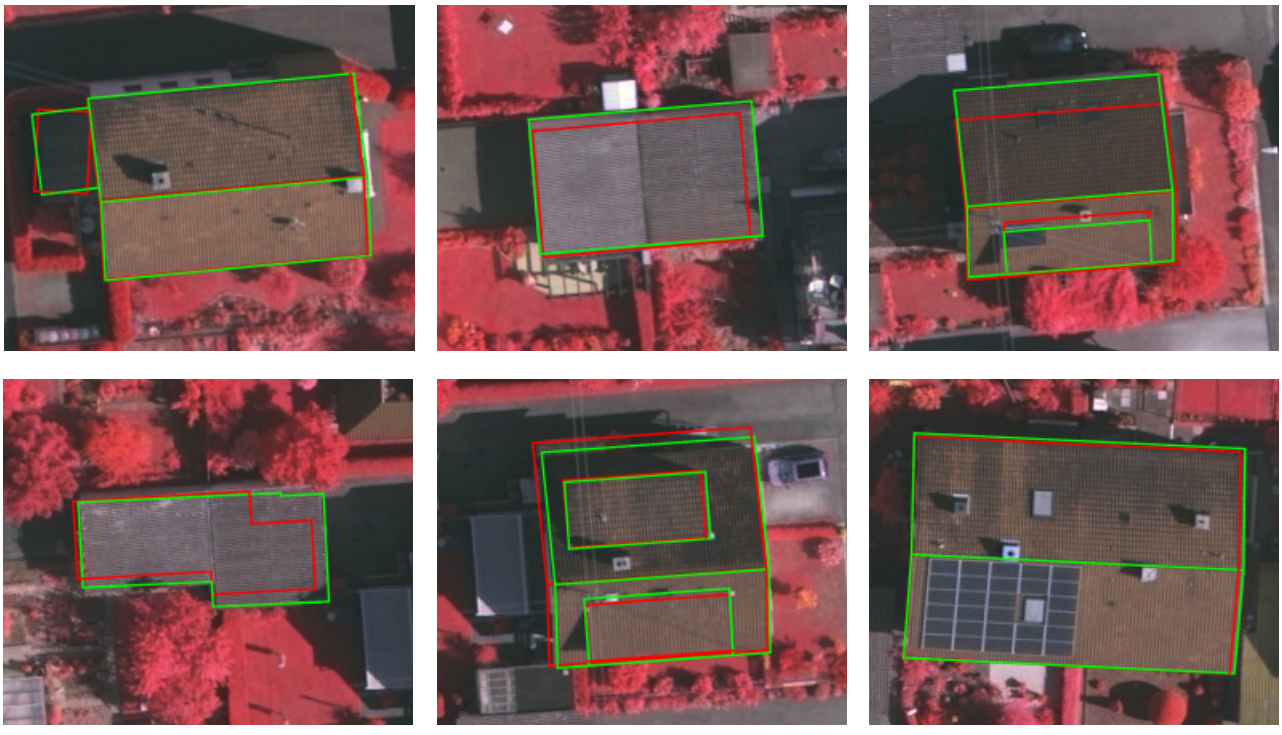

Figure 3. Comparison of building roof edges before (red) and after refinement (green).

indicators computed per-area level are not expected to highly change. As shown in a table, an average RMS error calculated with respect to the reference boundaries is reduced by 9 cm (from 73 cm to 64 cm). Positive impact of the refinement procedure on the final results is also revealed in coverage evaluation. The sum of True Positive area increased from 7430 m^2 to 7522 m^2, while False Positive indicator decreases from 684 m^2 to 592 m^2. A significant improvement of the refined models geometry is also confirmed by visual comparison of building edges already presented in Fig.1. Especially for instances, where large positional deviations occur (c.f. Fig.3) integration of optical imagery compensates for reconstruction drawbacks and leads to more accurate building models.

4. CONCLUSIONS

We have presented a method for sequential refinement of ALS-based building models using single aerial image. The novelty of the proposed reconstruction approach is to extract refined roof corners by direct intersection of 3D roof planes previously detected from laser scanning data with viewing planes assigned to roof edges and extracted from single image. The methodology enables us to benefit from the synergy between LiDAR and optical imagery in the context of high vertical and plannimetric accuracy. Integration of linear cues retrieved from imagery allowed for an average improvement of planar accuracy by 9 cm (RMS error calculated for roof plane outlines). Visual comparison of the refinement performance indicates that the refinement impact is not distributed regularly. For many instances substantial edge correction is not needed; however in case of large positional deviations the applied refinement clearly compensates reconstruction drawbacks. In this preliminary study, we confirmed that the proposed approach is able to improve the geometric accuracy of 3D building models. The underlying methodology so far assumes that the structural arrangements of model edges reconstructed from ALS data is topologically correct. In the future work we will extend the range of the refinement by a possibility for modification of a model shape and on the simultaneous use of multiple aerial images.

ACKNOWLEDGEMENTS

This work was supported by National Science Centre, Poland (Project No 2014/13/N/ST10/04892). The Vaihingen data set was provided by the German Society for Photogrammetry, Remote Sensing and Geoinformation (DGPF) http://www.ifp.uni-stuttgart.de/dgpf/DKEP-Allg.html. The authors wish to thank the chair persons of ISPRS Commission III/4 for the evaluation of the results.

REFERENCES

Bulatov, D., Haufel, G., Meidow, J., Pohl, M., Solbrig, P., Wernerus, P., 2014. Context based automatic reconstruction and texturing of 3D urban terrain for quick response tasks. ISPRS Journal of Photogrammetry and Remote Sensing 93, 157–170.

Chen, L., Teo, T., Rau, J., Liu, J., Hsu, W., 2005. Building reconstruction from LiDAR data and aerial imagery. Proceedings of the IEEE International Geoscience and Remote Sensing Symposium, vol. 4. pp. 2846 – 2849.

Dal Poz, A. P., 2014. Synergy Between LiDAR and Image Data in Context of Building Extraction, The International Archives of the Photogrammetry, Remote Sensing and Spatial Information Sciences, Vol. XL-1, pp. 89-93.

Demir, N. and Baltsavias, E., 2012. Automated modeling of 3D building roofs using image and LiDAR data. ISPRS Annals of the Photogrammetry, Remote Sensing and Spatial Information Sciences, Vol. I-4, pp.35-40.

Habib, A., Kwak, E., Al-Durgham, M., 2011. Model-based automatic 3D building model generation by integrating LIDAR and aerial images. Archives of Photogrammetry, Cartography and Remote Sensing, Vol. 22, 2011, pp. 187-200

Jarząbek-Rychard M., Borkowski A., 2016. 3D building reconstruction from ALS data using unambiguous decomposition into elementary structures. ISPRS Journal of Photogrammetry and Remote Sensing, vol. 118, pp. 1-12.

Kim, K., Shan, J., 2011. Building roof modeling from airborne laser scanning data based on level set approach. ISPRS Journal of Photogrammetry and Remote Sensing 66, pp.484-497.

Nex, F., Remondino, F. 2012: Automatic roof outlines reconstruction from photogrammetric DSM. Annals of the Photogrammetry, Remote Sensing and Spatial Information Sciences, Vol. I(3), pp. 257-262

Oude Elberink, S., Vosselman, G., 2009. Building reconstruction by target based graph matching on incomplete laser data: analysis and limitations. Sensors 9, pp. 6101–6118.

Perera, G.S.N., 2014. Automated generation of 3D building models from dense point clouds & aerial photos. PhD Thesis, TU Dresden

Rottensteiner, F., Sohn, G., Gerke, M., Wegner, J.-D., Breitkopf, U., Jung, J., 2014. Results of the ISPRS benchmark on urban object detection and 3D building reconstruction. ISPRS Journal of Photogrammetry and Remote Sensing, Volume 93, 256-271.

Rutzinger, M., Rottensteiner, F., Pfeifer, N., 2009. A comparison of evaluation techniques for building extraction from airborne laser scanning. IEEE Journal of Selected Topics in Applied Earth Observations & Remote Sens. 2 (1), 11–20.

Sohn, G., Jung, J., Jwa, Y., and Armenakis, C., 2013. Sequential modelling of building rooftops by integrating airborne LiDAR data and optical imagery: preliminary results, ISPRS Annals of the Photogrammetry, Remote Sensing and Spatial Information Sciences, vol. II-3/W1, pp. 27-33.

Xiong, B.; Jancosek, M.; Oude Elberink, S.; Vosselman, G., 2015. Flexible building primitives for 3D building modeling. ISPRS Journal of Photogrammetry and Remote Sensing, Vol. 101, pp. 275–290.

Zhang, W., Wang, H., Chen, Y., Yan, K., Chen, M., 2014. 3D Building Roof Modeling by Optimizing Primitive's Parameters Using Constraints from LiDAR Data and Aerial Imagery. Remote Sensing 6 (9), 8107-8133.